JACS
JOURNAL OF THE AMERICAN CHEMICAL SOCIETY
Article
pubs.acs.org/JACS

Multiple Shape Transformations of Composite Hydrogel Sheets

Héloïse Thérien-Aubin,[‡] Zi Liang Wu,[‡] Zhihong Nie,*[,§] and Eugenia Kumacheva*[,‡]

[‡]Department of Chemistry, University of Toronto, 80 Saint George Street, Toronto, Ontario M5S 3H6
[§]Department of Chemistry and Biochemistry, University of Maryland, College Park, Maryland 20742, United States

Supporting Information

ABSTRACT: Soft materials undergoing shape transformations in response to changes in ambient environment have potential applications in tissue engineering, robotics and biosensing. Generally, stimulus-responsive materials acquire two stable shapes corresponding to the "on" and "off" states of the external trigger. Here, we report a simple, yet versatile approach to induce multiple shape transformations of a planar hydrogel sheet, each triggered by a particular, well-defined external stimulus. The approach is based on the integration of small-scale multiple polymer components with distinct compositions in the composite gel sheet. In response to different stimuli, the structural components undergo differential swelling or shrinkage, which creates internal stresses within the composite hydrogel sheet and transforms its shape in a specific manner.

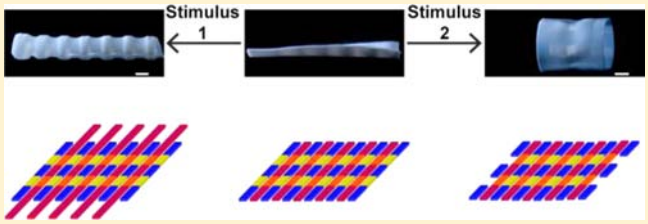

INTRODUCTION

Over the past decade, substantial progress has been achieved in the design and development of polymer materials that change their properties and performance in response to the change in ambient conditions.[1−4] Generally, adaptable materials have been designed to respond to a particular, well-defined external stimulus such as heat, light, or the variation in humidity, acidity and ionic strength of the surrounding medium.[5−7] Multiplexing system's functionality is an appealing concept that enables the design of materials with multiple, distinct properties, each of which is activated by a particular external trigger. One approach to multiplexing builds on the integration of multiple, small-scale structural and/or compositional components in a macroscopic material. An appropriate selection of structural components offers the ability to program the ultimate response of the system to multiple external triggers. An exemplary system is a multiphase, nanostructured polymer film containing ultraviolet, visible and infrared dyes that are localized in the different phases of the film. Selective photobleaching of each dye at a particular, dye-specific wavelength enables up to eight (2^3) recording modalities.[8,9] Each of the recorded patterns can be selectively retrieved by irradiating the film at the corresponding wavelength, thereby paving the way for high-density optical data storage and biometric applications.

When the material's response to the external trigger is reversible, the system can adjust its properties to the changes in ambient environment. Such adaptability is frequently encountered in nature, e.g., humidity mediated change in shape of plant organs such as pine cones or valves of peapods.[10−15] Influx and efflux of water in and out of the plant tissue leads to differential swelling along or across the plant organ and results in build-up of internal stresses, which, in turn, cause its reversible shape changes.

Morphogenesis of plant tissues that is driven by the distribution of stresses has largely motivated recent studies of three-dimensional (3D) shape transformations of composite polymer sheets.[16−27] For example, planar-to-3D shape transitions were achieved by modulating a local concentration and/or cross-linking density of the temperature-responsive polymer in hydrogel sheets.[22−27] Upon heating, regions with different polymer contents underwent differential swelling, and in response to that, the sheet minimized its elastic energy by adopting a particular 3D morphology. The utilization of a single stimulus (the change in temperature) resulted in two stable shapes of the system, corresponding to the "on" and "off" states of the trigger.

In the present work, we report an approach to achieving multiple 3D shape transformations of planar gel sheets in response to distinct external triggers. We used a photolithographic method to combine multiple, small-scale structural components with different compositions in a planar gel sheet. Each component was 'programmed' to respond to a particular stimulus. In response to the change in temperature, pH, ionic strength, or supply of CO_2, the different regions of the sheet underwent site-specific swelling or contraction, thereby generating within the sheet localized internal stresses. Since each structural component was responsive to a particular external trigger, the build-up of stresses led to a distinct shape transformation of the planar sheet. The cooperative response of the entire gel sheet to external stimuli, as well as the absence of cross-talk between the components, was achieved by combining polymers with particular compositions, thereby achieving an optimized mismatch in their swelling and elastic properties.

Received: January 16, 2013
Published: March 6, 2013

EXPERIMENTAL SECTION

Gel Synthesis. Composite patterned gel sheets were prepared by introducing a first monomer solution into a 6 in. × 3 in. reaction cell composed of two glass plates separated with a 0.44 mm-thick silicone rubber spacer. The cell was then exposed to UV-irradiation (Hönle UVA print 9 mW/cm^2) leading to the formation of the primary gel (PG). Following photopolymerization, the sheet of PG was cut into 3 in. × 2 in. pieces, which were washed in 750 mL of water for 24 h (changed every 8 h) and then swollen for 18 h in a 250 mL of a second aqueous monomer solution (see Supporting Information). The swollen gel was introduced into the reaction cell and exposed to UV-irradiation through a photomask printed on a transparency. The interpenetrating network (IPN) was formed in the light-exposed regions of the swollen gel, thereby forming the features of the binary gel (BG). The gel sheet was washed in 750 mL of water (changed every 8 h) for 24 h to remove unreacted reagents and linear, non-cross-linked polymers. The final thickness of the patterned gel was 0.44 ± 0.04 mm.

Gel Swelling. For each system used in the present work, disks were prepared from individual components of the patterned hydrogel sheets. The disks had a diameter of 1.27 cm and the thickness of 3.2 mm. The disks were incubated in water at pH = 6.5 for 24 h at room temperature (for poly(acrylamide-*co*-butyl methacrylate)/poly-methacrylic acid gels pH = 3 was used), and the dimensions of the disks, D_0, were measured. The disks were then immersed for 8 h in the solution with a particular pH, temperature or ionic strength used for gel actuation and the dimension of the disk, D_a, was measured again. The swelling ratio was determined as $\alpha = D_a/D_0$.

Mechanical Properties. An Instron 5848 Microtester was used to measure the Young's modulus of gel disks with a diameter of 1.32 cm and thickness of 0.44 mm.

RESULTS AND DISCUSSION

Preparation of the Composite Gel Sheets. Figure 1 illustrates the preparation of the composite gel. A thin sheet of the primary gel (PG) is prepared by redox, thermo- or photoinitiated polymerization (Figure 1a). The sheet is swollen with a solution containing a monomer, a photoinitiator and a cross-linking agent (Figure 1b). This solution may have a different or the same composition as the solution used for the preparation of PG and may contain dyes, inorganic nanoparticles or precursors for the synthesis of inorganic nanoparticles. The swollen PG sheet is exposed to UV-irradiation through a photomask, in order to initiate photopolymerization of the monomer in the light-exposed regions. The photomask contains black and transparent features or different shades of gray. Following photopolymerization, the light-exposed regions of the sheet contain a gel with an interpenetrating network (IPN) structure (or a binary gel, BG) (Figure 1c). The non-cross-linked polymer and the unreacted monomer from the light-protected regions are subsequently removed by washing the gel sheet in an appropriate solvent. The resulting composite gel (Figure 1d) contains PG and BG regions in the light-protected and light-exposed areas, respectively. Under external stimulus, these regions function as the distinct small-scale structural components of the composite gel. Steps b–d can be repeated to embed in the gel more than two structural components with different stimuli-responsive properties by using similar or different masks.

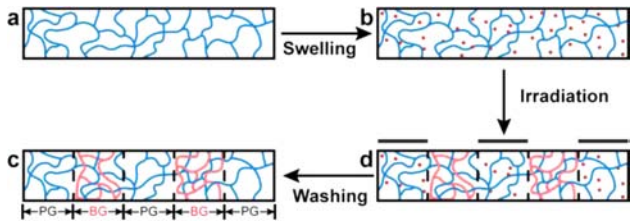

Figure 1. Schematic of the preparation of the composite gel sheet. A thin film of the primary hydrogel (PG) (a) is swollen with an aqueous solution of the monomer, photoinitiator and a cross-linking agent (b) and exposed to UV-irradiation through a photomask. The monomer solution is schematically shown with red circles. Photopolymerization leads to the formation of a binary gel (BG) in the light-exposed regions (c). After washing, a patterned gel contains the regions of PG and BG (d).

The photopatterning of the composite gel sheets has the following advantages: (i) it enables patterning of multiple regions of different stimuli-responsive homopolymers and copolymers in the gel film; (ii) it offers the ability to achieve large mismatches in swelling and mechanical properties of the structural components of the sheet; (iii) it provides a simple and versatile strategy for the patterning of arbitrary-shape features, with prospective applications of the composite gels in actuation, sensing and soft robotics.

To develop a rationale for combining particular PG and BG structural components with different swelling and elastic properties, we first, explored shape transformations of the composite hydrogel sheets under the action of a single external stimulus (Figure 2).

A PG disk of poly(*N*-isopropylamide) (PNIPAm) was patterned with features of poly(2-acrylamido-2-methylpropane) sulfonic acid (PAMPS), thereby forming PNIPAm/PAMPS BG

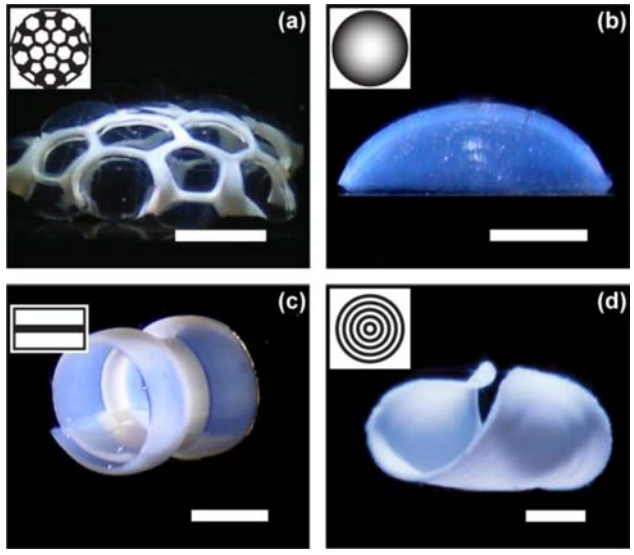

Figure 2. Three-dimensional configurations adopted by composite gel sheets under the action of various stimuli. (a and b) Dome-shape structures formed in a 1 M NaCl solution by PNIPAm/PAMPS hydrogel disks patterned using a photomask of 2D projection of a truncated icosahedron (a) or a photomask with a shade of gray increasing from the center to the circumference (b). (c) An hourglass structure generated in deionized water at 45 °C by a rectangular gel sheet composed of a central PNIPAm stripe and two outer PNIPAm/PNIPAm stripes. (d) A saddle-like structure formed by a P(AA-*co*-BMA) hydrogel disk patterned with circular rings of P(NIPAm-*co*-DMAEMA) when CO_2 is bubbled in the liquid medium. The insets show corresponding photomasks, in which the dark regions yield the regions of PG. The thickness of the gel films was 0.44 mm. The scale bars are 0.5 cm. In panels a and c, the white color corresponds to the strongly shrunk PG regions.

dx.doi.org/10.1021/ja400518c | *J. Am. Chem. Soc.* 2013, 135, 4834–4839

regions in the light-exposed areas (Figure 2a). A photomask used in this experiment was a 2D projection of a truncated isocahedron (Figure 2a, inset). Upon immersion of the composite planar gel sheet into a 1 M NaCl solution, the regions of PG underwent a strong contraction, due to the dehydration of the PNIPAm,[28] while the regions of BG remained highly swollen, due to the retention of water by PAMPS.[29] The mismatch in the dimensions and elastic properties of PG and BG regions led to the build-up of internal stresses. Figure 2a shows that the gel sheet adopted a dome shape with highly swollen transparent BG regions (pentagons and hexagons) and a collapsed PG skeleton (white regions).

In another approach to planar-to-dome shape transformations, a disk of PNIPAm (PG) was patterned with regions of PNIPAm/PAMPS (BG) by using a circular photomask with a gradual increase in shade of gray from the center of the circle to its circumference (Figure 2b). Photopolymerization led to the formation of the gradient gel with the concentration of PAMPS reducing from the center to the circumference of the disk. Upon exposure of the gel to a 1 M NaCl solution, the outer PAMPS-deprived region of the disk underwent a stronger shrinkage than the central, strongly swollen PAMPS-rich region. The nonuniform contraction along the radial direction of the disk induced buckling which led to a planar-to-dome transition.

In the second series of experiments, we induced the change in shape of a rectangular PNIPAm sheet containing regions with a different polymer concentration and a cross-linking density. A PNIPAm sheet was swollen with a solution of *N*-isopropylamide, a photoinitiator and a cross-linking agent and exposed to UV-irradiation through a mask: a dark central stripe and two outer transparent areas (Figure 2c, inset). The resultant gel sheet contained a central PNIPAm PG stripe and two outer PNIPAm/PNIPAm BG stripes with the average polymer content of 13 and 17 wt %, respectively. Upon heating of the patterned gel to 45 °C in deionized water, above the lower critical solution temperature (LCST) of PNIPAm, the polymer chains collapsed through cooperative dehydration.[30,31] The central PG region exhibited stronger shrinkage than the two outer BG domains. In response to the stress created by the localized shrinkage of the PG region, the hydrogel sheet adopted an hourglass shape (Figure 2c), as observed and predicted in previous works.[23,25]

Figure 2d illustrates shape transformation of a poly(acrylamide-*co*-butylmethacrylate) (P(AA-*co*-BMA)) gel disk patterned with concentric rings of poly(NIPAm-*co*-dimethylamino-ethylmethacrylate) (P(NIPAm-*co*-DMAEMA)). The P(AA-*co*-BMA) and P(NIPAm-*co*-DMAEMA)/P(AA-*co*-BMA) regions formed PG and BG circles, respectively. Purging of the CO_2 gas through the system led to the reduction of pH from 6.8 to 3.9, caused by the reaction of CO_2 with water. The BG regions swelled, due to the ionization of amino groups,[32] while the dimensions of the PG regions did not notably change. The composite gel acquired a saddle shape, which was predicted and experimentally realized for non-Euclidean plates formed by thick hydrogel disks with differential swelling in the radial direction.[24−26]

Generally, the planar-to-3D shape transitions became apparent 5−30 min after immersion of the composite gel sheets in the actuation solution, and the shape reached an equilibrium state in 6−8 h. The rate of shape transformation was governed by diffusion of the solution in and out of the hydrogel sheet. All shape transitions illustrated in Figure 2 were reversible with respect to the stimulus applied. Complete recovery of the sheet shape and no hysteresis were observed for, at least, 10 actuation cycles. For example, the saddle shape configuration completely relaxed to a planar sheet by purging the system with Ar gas, thereby removing CO_2 from the liquid environment.

Shape transformations shown in Figure 2 originated from the difference in swelling and elastic properties of the structural components of the composite gel under the action of external stimulus.[23−25,27] Since the regions of PG and BG were connected, the shrinkage or swelling of the actuated (active) gel forced the neighboring region to change its original dimensions and shape, thereby generating stress in the hydrogel sheet. The stress could be relaxed by reducing the bending and stretching energies of the sheet.

The stretching energy of the soft sheet scales as $E_S \sim (\delta/L)^2 t$, where t is the thickness of the sheet, δ the deformation, and L is the original domain size,[25] while the bending energy of the sheet scales as $E_B \sim kt^3$, where k is the curvature of the sheet.[25] In our work, the shape of the composite hydrogel films was determined by the competition of bending and stretching energies, and the composite hydrogel sheet relaxed the stress by buckling to acquire the shape with a particular curvature.

For example, the formation of the dome structure shown in Figure 2a was governed by the cooperative internal stresses generated in the disk, due to the mismatch in the swelling and elastic moduli of the PNIPAm (PG) and PNIPAm/PAMPS (BG) regions. In a 1 M NaCl solution, the swelling ratios were 0.6 and 1.35 and the measured Young's moduli were 1.3 and 0.27 MPa for PG and BG, respectively. To minimize its elastic energy and reduce the strain, the gel disk buckled. The curvature of the dome was determined by the competition between the bending and stretching energies of the system.[25,26]

To achieve 3D shape transformations of the composite gel sheets, the swelling and elastic properties of the PG and BG regions had to be optimized. Figure 3 shows shape transformations of the exemplary gel sheet composed of P(AA-*co*-BMA) (PG) stripes and P(AA-*co*-BMA)/PNIPAm (BG) stripes (Table S1, Supporting Information shows the optimized

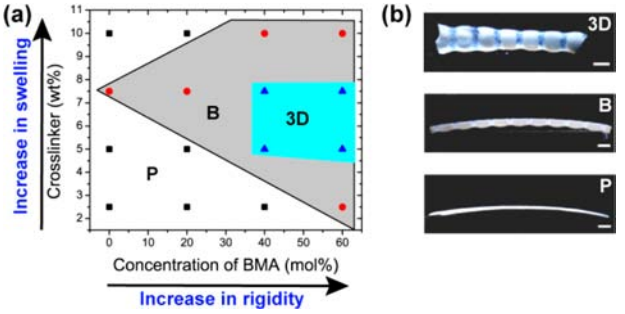

Figure 3. Effect of the composition of P(AA-*co*-BMA)/PNIPAm gel on shape transitions of the composite sheet in a 1 M NaCl solution. (a) Phase-like diagram of shape transformations of the composite gel, including a planar gel shape (P), a buckled gel shape (B) and a transformation to a roll (3D). (b) Photographs of the gel sheets in different configurations. The labels P, B and 3D correspond to the regimes specified in panel a. The scale bars are 0.5 cm. The 0.44 mm-thick hydrogel sheet was patterned with 4 mm-wide stripes of P(AA-*co*-BMA) and 1 mm-wide stripes of P(AA-*co*-BMA)/PNIPAm. Both types of stripes were oriented perpendicular to the long axis of the sheet. The white regions correspond to the PG domains.

dx.doi.org/10.1021/ja400518c | *J. Am. Chem. Soc.* 2013, 135, 4834−4839

swelling ratios for other PG and BG combinations), where the stress created by the shrinkage of the PNIPAm-containing domains led to the formation of a cylindrical tube. We varied the content of the BMA comonomer in the P(AA-*co*-BMA) component of the gel and the concentration of the cross-linking agent methylene-*bis*-acrylamide (MBA) in BG regions. Upon incubation in a 1 M NaCl solution, a planar-to-roll transition (labeled as "3D" in Figure 3a) occurred in a particular range of concentrations of MBA and BMA. The rigidity of the P(AA-*co*-BMA) regions (tuned by the varying content of BMA) was "balanced" by their ability to shrink under the influence of the collapsed PNIPAm network, which was controlled by varying the concentration of MBA. Too rigid P(AA-*co*-BMA) regions with a higher content of BMA did not comply to the stress imposed by the shrinkage of the adjacent P(AA-*co*-BMA)/PNIPAm BG stripes. On the other hand, excessively soft PG regions were easily deformed by the collapsed BG regions, without a significant stress build-up at the domain interface. Under these two conditions, the gel sheet retained its planar configuration or exhibited limited buckling (labeled as "P" and "B", respectively, in Figure 3). In addition, composite gels containing rigid and strongly swelling PG showed a trend to crack at the PG−BG interface after incubation in actuation solution. This effect originated from the inability of the system to release the stress by bending and buckling.

While conceptually our approach to shape transformations of planar gel sheets resembled halftone gel lithography method,[27] the critical difference was that its ability to generate in a planar gel multiple small-scale regions with *different* compositions. Each of these regions could be activated by a distinct, well-defined stimulus, leading to the design of polymer systems with more than two stable shapes adopted under actuation.

We explored this concept by designing a sheet that combined two structural hydrogel components with different values of LCST. Periodic stripes of poly(hydroxyl ethylacrylamide-*co*-*N*-isopropylacryl-amide) (P(HEAm-*co*-NIPAm) and (P(HEAm-*co*-NIPAm)/PNIPAm hydrogels were integrated in the gel sheet as PG and BG regions, respectively . Table 1 shows the values of LSCT of these hydrogels. The copolymer of NIPAm and HEAm (PG) was more hydrophilic than PNIPAm, and its LCST shifted to 50 °C. The P(NIPAm-*co*-HEAm)/PNIPam BG hydrogel exhibited two values of LCST. The first one at 35 °C was associated with dehydration of the PNIPAm network and the second one at 55 °C was associated with the collapse of P(NIPAm-co-HEAm) copolymer.

Table 1. Properties of Two-Component Composite Hydrogel

structural component of the gel sheet	composition	LCST (°C)	α^a	α^b
PG	P(HEAm-*co*-NIPAm)	50	0.94	0.31
BG	P(HEAm-*co*-NIPAm)/PNIPAm	35 55	0.65	0.38

[a]Swelling ratio, α, was determined as the ratio of gel dimensions at 40 and 25 °C (corresponding to the transition from Figure 4a to Figure 4b). [b]Swelling ratio, α, was determined as the ratio of gel dimensions at 65 °C and the unperturbed system at 25 °C (corresponding to the transition from Figure 4a to Figure 4c).

In the composite gel, the stripes of PG and BG passed at an angle of 45° with respect to the long axis of the rectangular sheet. At 25 °C, the PG and BG stripes had similar dimensions, resulting in a planar shape of the gel (Figure 4a). Heating the sheet to 40 °C (above the first LCST of BG of 35 °C) led to the shrinkage of BG stripes at the swelling ratio of 0.65 (Table 1), while the PG stripes maintained their close-to-initial dimensions, thereby building stresses in the composite sheet. Under these conditions, the planar sheet transformed into a helix (Figure 4b, right) with a pitch of 2.7 cm. Next, we heated the sheet to 65 °C, above the LCST of PG of 50 °C (and the second LSCT of BG of 55 °C). The difference in dimensions between the PG and BG stripes diminished (the corresponding swelling ratio were 0.38 and 0.31, respectively), thereby triggering a helical-to-planar transition (Figure 4c) of the sheet. Thus, the composite sheet exhibited three stable states at three distinct temperatures.

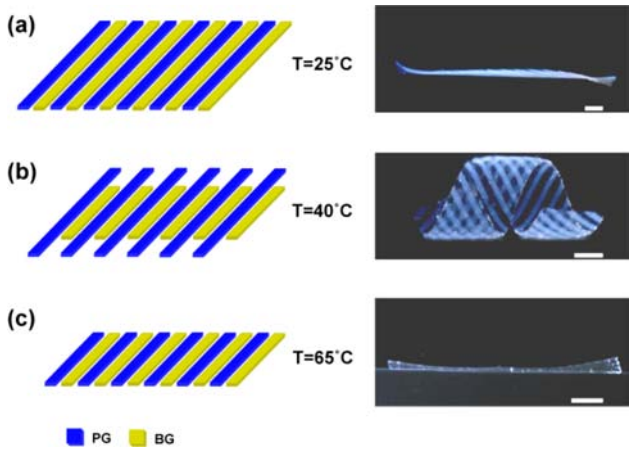

Figure 4. Shape transformations of the gel sheet composed of P(NIPAm-*co*-HEAM) (PG) and poly(NIPAM-*co*-HEAM)/PNIPAm (BG) stripes. (a) At 25 °C, PG and BG regions have similar dimensions (left) and the gel acquires a planar shape (right). (b) At 45 °C, the BG regions shrink (left), and the gel adopts a helical shape (right). (c) At 65 °C, the PG and BG regions both shrink to the same extent (left) and the sheet returns to a planar conformation (right). The thickness of the hydrogel was 0.44 mm. The PG and BG stripes were 1 mm-wide and were oriented at 45° to the long axis of the rectangular gel sheet. The scale bars are 0.5 cm.

To achieve more complex multiple shape transformations of the composite gel sheet, we combined in the composite gel sheet three structural components that exhibited a different extent of shrinkage/swelling at a particular pH and ionic strength of the surrounding medium (Table 2). We selected a P(AA-*co*-BMA) copolymer gel as a neutral PG "host" and patterned it, first, with stripes of poly(methacrylic acid)

Table 2. Properties of Three-Component Hydrogel

structural component of the gel sheet	composition	α^a	α^b
PG	P(AA-*co*-BMA)	1.02	1.05
BG-1	P(AA-*co*-BMA)/PMAA	1.11	3.2
BG-2	P(AA-*co*-BMA)/PNIPAm	0.47	0.92

[a]The swelling ratio, α (corresponding to the transition from Figure 5a to Figure 5c), was determined at pH = 4 as the ratio of gel dimensions at [NaCl] = 1.5 M and at [NaCl] = 0. [b]The swelling ratio, α (corresponding to the transition from Figure 5a to Figure 5b), was determined at [NaCl] = 0 as the ratio of gel dimensions at pH = 9.5 and pH = 4.

dx.doi.org/10.1021/ja400518c | J. Am. Chem. Soc. 2013, 135, 4834−4839

(PMAA), thereby forming a P(AA-*co*-BMA)/PMAA IPN gel (denoted as BG-1). In the second step, we patterned the host gel with PNIPAm stripes, thereby creating P(AA-*co*-BMA)/PNIPAm IPN regions (denoted as BG-2). The compositions of BG-1 and BG-2 were such that BG-1 swelled at pH > 7.3 (above the pK_a value of PMAA),[33] and BG-2 shrank in a solution of high ionic strength, due to the dehydration of the PNIPAm chains.[28] The swelling curves are shown in Figures S1 and S2. The swelling ratios of PG, BG-1 and BG-2 are shown in Table 2. At pH = 9.5, the BG-1 domains swelled and the PG and BG-2 domains remain almost intact, while at high ionic strength, the BG-2 domains collapsed and the PG and BG-1 domains were unaffected.

In the composite hydrogel sheet, the stripes of BG-1 and BG-2 were oriented at 0 and 90° to the long axis of the rectangular gel sheet, respectively (Figure 5a–c, left), which dictated the shape of the composite gel adopted under a particular stimulus, that is, the change in pH of the medium or addition of NaCl.

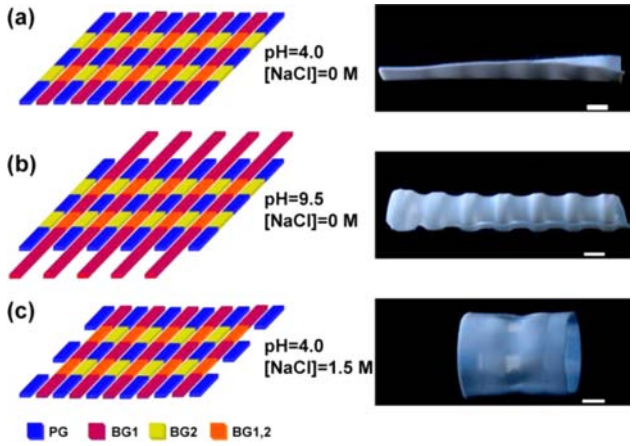

Figure 5. Multiple shape transformations of the composite gel sheets. (a) At pH = 4 and [NaCl] = 0 in the as-prepared hydrogel sheet, both PG and BG-2 regions are swollen and the BG-1 regions are in the unswollen (shrunk) state (left). The gel sheet acquires a planar shape. (b) At pH = 9.5 and [NaCl] = 0, the BG-1 regions swell (left) and the regions of BG-2 and PG keep their unperturbed dimensions, leading to the formation of a long cylinder (right). (c) At pH = 4 and [NaCl] = 1.5 M, the BG-2 regions collapse, while the PG and BG-1 domains have dimensions identical to as-prepared hydrogel sheet (left). The gel sheet adopts a drum shape (right). The thickness of the rectangular hydrogel sheet is 0.44 mm and the BG-1 and BG-2 stripes are oriented at 90 and 0° to the long axis of the gel sheet, respectively. The scale bars are 0.5 cm.

Figure 5 shows shape transformations of the composite gel sheet patterned with perpendicularly oriented BG-1 and BG-2 stripes. At pH = 4 and [NaCl] = 0, in the as-prepared hydrogel sheet, the PG, BG-1 and BG-2 regions had similar dimensions, due to the swollen state of PG and BG-2 and the unswollen (shrunk) state of BG-1 (Figure 5a, left). This was the reference state of the system, in which the sheet adopted a close-to-planar shape (Figure 5a, right). Under basic conditions (pH = 9.5, [NaCl] = 0), the PG and BG-2 domains maintained their close-to-original dimensions (the swelling ratios were 1.05 and 0.92, respectively, Table 2), while the BG-1 stripes were oriented perpendicular to the long axis of the sheet swelled (the swelling ratio was 3.2). The hydrogel sheet transformed from a flat shape to a long tight cylinder (Figure 5b, right). Under high ionic strength conditions ([NaCl] = 1.5 M, pH = 4), the BG-2 regions that were oriented parallel to the long axis of the sheet shrank, while the PG and BG-1 domains maintained their original dimensions (the swelling ratios were 1.02 and 1.11, respectively). Under these conditions, the planar sheet formed as loose roll (Figure 5c, right). Importantly, during actuation, the counterpart components of the actuated gel region were not chemically active, that is, the cross-talk between them was eliminated. Thus, the composite gel sheet selected one of the three shapes, each of which was dictated by the external stimulus.

CONCLUSIONS

In summary, we developed a new, efficient approach to the generation of composite gel sheets that are preprogrammed to acquire a particular, well-defined shape under the action of a particular external trigger. The use of the photopatterning method and the combination of small-scale homopolymer and copolymer structural components enabled the design of gel sheets capable of large 3D shape transitions. This work paves the way for producing multiresponsive adaptable materials (programmable matter), with potential applications in soft robotics, actuation and sensing.

ASSOCIATED CONTENT

Supporting Information

Gel syntheses and swelling behavior. This material is available free of charge via the Internet at http://pubs.acs.org.

AUTHOR INFORMATION

Corresponding Author

znie@umd.edu; ekumache@chem.utoronto.ca

Notes

The authors declare no competing financial interest.

ACKNOWLEDGMENTS

E.K. thanks NSERC Canada (Discovery Grant and Canada Research Chair program) for financial support of this work. Z.N. thanks the support of startup funds from the University of Maryland.

REFERENCES

(1) Capadona, J. R.; Shanmuganathan, K.; Tyler, D. J.; Rowan, S. J.; Weder, C. *Science* **2008**, *319*, 1370–1374.
(2) He, X. M.; Aizenberg, M.; Kuksenok, O.; Zarzar, L. D.; Shastri, A.; Balazs, A. C.; Aizenberg, J. *Nature* **2012**, *487*, 214–218.
(3) Suo, Z. G. *MRS Bull.* **2012**, *37*, 218–225.
(4) Ravichandran, R.; Sundarrajan, S.; Venugopal, J. R.; Mukherjee, S.; Ramakrishna, S. *Macromol. Biosci.* **2012**, *12*, 286–311.
(5) Stuart, M. A. C.; Huck, W. T. S.; Genzer, J.; Muller, M.; Ober, C.; Stamm, M.; Sukhorukov, G. B.; Szleifer, I.; Tsukruk, V. V.; Urban, M.; Winnik, F.; Zauscher, S.; Luzinov, I.; Minko, S. *Nat. Mater.* **2010**, *9*, 101–113.
(6) Luzinov, I.; Minko, S.; Tsukruk, V. V. *Prog. Polym. Sci.* **2004**, *29*, 635–698.
(7) Kim, P.; Zarzar, L. D.; He, X. M.; Grinthal, A.; Aizenberg, J. *Curr. Opin. Solid State Mater. Sci.* **2011**, *15*, 236–245.
(8) Gourevich, I.; Pham, H.; Jonkman, J. E. N.; Kumacheva, E. *Chem. Mater.* **2004**, *16*, 1472–1479.
(9) Pham, H. H.; Gourevich, I.; Oh, J. K.; Jonkman, J. E. N.; Kumacheva, E. *Adv. Mater.* **2004**, *16*, 516–520.
(10) Cook, T. A. *The Curve of Life*; Constable: London, 1914.
(11) Dawson, C.; Vincent, J. F. V.; Rocca, A.-M. *Nature* **1997**, *390*, 668–668.
(12) Fratzl, P.; Barth, F. G. *Nature* **2009**, *462*, 442–448.

(13) Harrington, M. J.; Razghandi, K.; Ditsch, F.; Guiducci, L.; Rueggeberg, M.; Dunlop, J. W. C.; Fratzl, P.; Neinhuis, C.; Burgert, I. *Nat. Commun.* **2011**, *2*, 337.
(14) Armon, S.; Efrati, E.; Kupferman, R.; Sharon, E. *Science* **2011**, *333*, 1726−1730.
(15) Ionov, L. *J. Mater. Chem.* **2012**, *22*, 19366−19375.
(16) Hu, Z.; Zhang, X.; Li, Y. *Science* **1995**, *269*, 525−527.
(17) Zhang, J. J.; Wu, J. J.; Sun, J. Z.; Zhou, Q. Y. *Soft Matter* **2012**, *8*, 5750−5752.
(18) Yang, S.; Khare, K.; Lin, P. C. *Adv. Funct. Mater.* **2010**, *20*, 2550−2564.
(19) Bassik, N.; Abebe, B. T.; Laflin, K. E.; Gracias, D. H. *Polymer* **2010**, *51*, 6093−6098.
(20) Shim, T. S.; Kim, S.-H.; Heo, C.-J.; Jeon, H. C.; Yang, S.-M. *Angew. Chem., Int. Ed.* **2012**, *51*, 1420−1423.
(21) Ionov, L. *Soft Matter* **2011**, *7*, 6786−6791.
(22) Zhang, X.; Pint, C. L.; Lee, M. H.; Schubert, B. E.; Jamshidi, A.; Takei, K.; Ko, H.; Gillies, A.; Bardhan, R.; Urban, J. J.; Wu, M.; Fearing, R.; Javey, A. *Nano Lett.* **2011**, *11*, 3239−44.
(23) Kim, J.; Hanna, J. a.; Hayward, R. C.; Santangelo, C. D. *Soft Matter* **2012**, *8*, 2375−2375.
(24) Klein, Y.; Efrati, E.; Sharon, E. *Science* **2007**, *315*, 1116−1120.
(25) Sharon, E.; Efrati, E. *Soft Matter* **2010**, *6*, 5693−5704.
(26) Klein, Y.; Venkataramani, S.; Sharon, E. *Phys. Rev. Lett.* **2011**, *106*, 118303.
(27) Kim, J.; Hanna, J. A.; Byun, M.; Santangelo, C. D.; Hayward, R. C. *Science* **2012**, *335*, 1201−1205.
(28) Schild, H. G. *Prog. Polym. Sci.* **1992**, *17*, 163−249.
(29) Kabiri, K.; Zohuriaan-Mehr, M.; Mirzadeh, H.; Kheirabadi, M. *J. Polym. Res.* **2010**, *17*, 203−212.
(30) Tanaka, T.; Sato, E.; Hirokawa, Y.; Hirotsu, S.; Peetermans, J. *Phys. Rev. Lett.* **1985**, *55*, 2455−2458.
(31) Zhang, X. Z.; Wu, D. Q.; Chu, C. C. *Biomaterials* **2004**, *25*, 3793−3805.
(32) Han, D.; Tong, X.; Boissière, O.; Zhao, Y. *ACS Macro Lett.* **2012**, *1*, 57−61.
(33) Ikawa, T.; Abe, K.; Honda, K.; Tsuchida, E. *J. Polym. Sci., Part A: Polym. Chem.* **1975**, *13*, 1505−1514.